TECHNICAL ARTICLE

Crystallographic structure of $LiFe_{1-x}Mn_xPO_4$ solid solutions studied by neutron powder diffraction

X.Y. Li, B. Zhang, Z.G. Zhang, L.H. He, H. Li, X.J. Huang, and F.W. Wang[a)]
Beijing National Laboratory for Condensed Matter Physics, Institute of Physics, Chinese Academy of Sciences, Beijing 100190, China

(Received 27 August 2013; accepted 19 December 2013)

High-resolution neutron powder diffraction (NPD) data were recorded on a series of cathode material $LiFe_{1-x}Mn_xPO_4$ ($x = 0$, 0.2, 0.5, 0.8, and 1.0) solid solutions using the HRPD machine at SINQ/PSI, Switzerland. *Ab initio* crystal structure solution via program FOX indicates demonstrably that the space group of $LiFePO_4$ is *Pnma* with Li^{1+} occupying octahedral (4a) sites and Fe^{2+} octahedral (4c) sites, respectively, in the olivine structure. Rietveld refinement (program FullProf suite version July-2011), complementary with X-ray diffraction data, shows that Fe^{2+} may partially (about 2%) distribute over Li^{1+} sites. NPD data for $LiFe_{1-x}Mn_xPO_4$ ($x = 0$, 0.2, 0.5, 0.8, and 1.0) reveal that the Mn^{2+} replaces Fe^{2+} at the octahedral (4c) sites. The cell parameters *a*, *b*, and *c* increase linearly and the interatomic distances (in Å) of Li–O(2) and Li–O(1) increase, while the interatomic distances (in Å) of Li–O(3) decrease on the addition of Mn, respectively, partially explaining a higher potential plateau of ~4.1 eV in $LiMnPO_4$ compared to ~3.5 eV in $LiFePO_4$. © *2014 International Centre for Diffraction Data*. [doi:10.1017/S0885715614000116]

Key words: $LiFe_{1-x}Mn_xPO_4$ compounds, neutron diffraction, *ab initio*

PACS: 82.47.Aa, 61.05.fm, 31.15.A-

I. INTRODUCTION

Lithium-ion batteries of lithium-insertion compounds as cathode materials, which are mainly used in portable electronics and electric transportation in the contemporary era, continue to gain extensively in scientific and commercial importance. These cathode materials should have high-energy density, high rate capability, be environmentally friendly, inexpensive, safe, and sustainable (Tarascon and Armand, 2001; Armand and Tarascon, 2008). It is widely recognized that the olivine-based phosphate family $LiMPO_4$ (M = Fe, Mn, Co, or Ni) (Padhi *et al.*, 1997a, 1997b) is an environmentally friendly cathode material for rechargeable lithium-ion batteries, particularly for the hybrid electric vehicles. $LiFePO_4$ shows a flat voltage curve with a plateau about 3.5 V (Padhi *et al.*, 1997a, 1997b; Yamada *et al.*, 2001) corresponding to the Fe^{3+}/Fe^{2+} redox energy and a theoretical capacity of 170 mAh g^{-1}. However, $LiFePO_4$ has a key limitation, an extremely low electronic conductivity because of its insulating nature. One method to increase $LiFePO_4$ conductivity is through the efficient formation of carbon-coated small particles (Dominko *et al.*, 2001; Huang *et al.*, 2001; Chung *et al.*, 2002); another method is the perturbative amount of supervalent cation M ($M = Mg^{2+}$, Al^{3+}, Ti^{4+}, Zr^{4+}, Nb^{5+}, and W^{6+}) into the Li site together with the point defects and partial replacement of Fe^{2+}/Fe^{3+} by some other transition metals of the type Mn, Co, Ni, or alkaline-earth metal Mg, etc. (Chung *et al.*, 2002; Morgan *et al.*, 2004; Wang *et al.*, 2005). In addition, Na-doping at Fe sites has also been purposed (Li *et al.*, 2009).

In the $LiMPO_4$ (M = Fe, Mn, Co, or Ni) olivine family, $LiFePO_4$ has the lowest operating potential, ~3.5 V vs. ~4.1 V for $LiMnPO_4$, ~4.8 V for $LiCoPO_4$, and ~5.2 V for $LiNiPO_4$, respectively (Padhi *et al.*, 1997a; Amine *et al.*, 2000; Li *et al.*, 2002; Zhou *et al.*, 2004; Wolfenstine and Allen, 2005). In $LiFe_{1-x}Mn_xPO_4$ solid solution, two plateaus at 3.5 and 4.1 V appeared on manganese doping. Molenda *et al.* (2007) revealed that the charge-transfer impedance in $Li_xFe_{1-y}Mn_yPO_4$ is much lower than that of Li_xFePO_4. Yao *et al.* (2006) revealed that the electrochemical performance of $LiFe_{1-x}Mn_xPO_4$ degrades with increasing Mn content.

Figure 1 shows the $LiFePO_4$ crystal structure of olivine-type with the oxygen atoms arranged in a hexagonal close-packed arrangement. The space group of $LiFePO_4$ is *Pnma* (Streltsov *et al.*, 1993; Padhi *et al.*, 1997a) with Li^{1+} occupying octahedral (4a) sites and Fe^{2+} octahedral (4c) sites, respectively, in the olivine structure. Neutron powder diffraction (NPD) patterns of $LiFe_{1-x}Mn_xPO_4$ ($x = 0$, 0.2, 0.5, 0.8, and 1.0) are shown in Figure 2. In this work, we investigate the crystallographic structure of $LiFe_{1-x}Mn_xPO_4$ in detail by high-resolution neutron diffraction, and attempt to define a relationship between the structure and electrochemical properties.

II. EXPERIMENTAL

$LiFe_{1-x}Mn_xPO_4/C$ was prepared by a solid-state reaction (Zhang *et al.*, 2010, 2011). Stoichiometric amounts of Li_2CO_3 (Shanghai China Lithium, 99.9%), $FeC_2O_4{\cdot}2H_2O$ (Hefei Yalong, 99%), $MnC_2O_4{\cdot}2H_2O$ (Hefei Yalong, 99%), $NH_4H_2PO_4$ (Beijing Chemical, 99.5%), the appropriate quantity of citric acid (Beijing Chemical, 99.5%) and sugar were mixed by using high-energy ball milling using a zirconia

[a)]Author to whom correspondence should be addressed. Electronic mail: fwwang@aphy.iphy.ac.cn

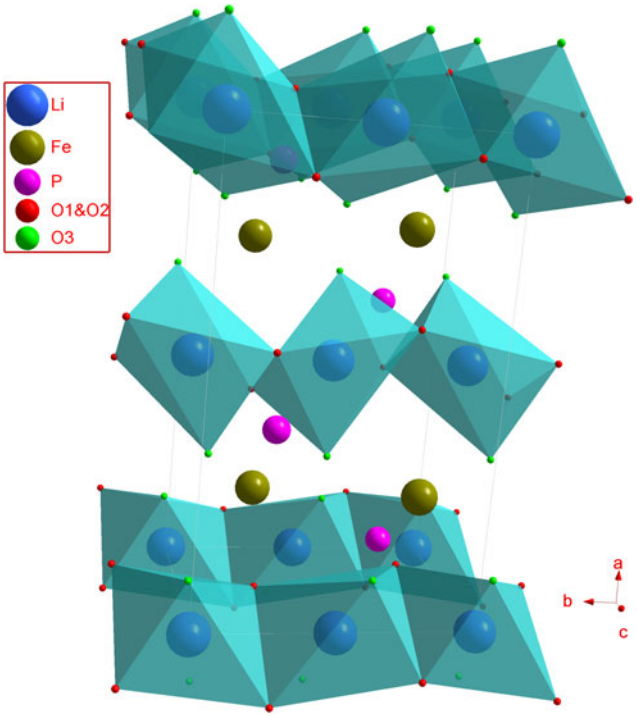

Figure 1. (Color online) The $LiFePO_4$ crystal structure of olivine-type.

container for 5 h. The mixture was then sintered at 650°C for 10 h under argon atmosphere (99.9999%). To confirm the chemical composition of these samples, the Fe/Mn ratios were determined using ICP (IRIS Intrepid II) after the complete dissolution of the powder into a hydrochloric acid solution. All samples are close to the target composition (Zhang *et al.*, 2010, 2011). The structure was analyzed by an X-ray diffraction (XRD) (Rigaku Rint-2400) with Cu$K\alpha$ radiation at a scan rate of 0.02° (2θ) s^{-1}.

Neutron diffraction was carried out on powder samples of $LiFe_{1-x}Mn_xPO_4$ ($x = 0$, 0.2, 0.5, 0.8, and 1.0) at room temperature on the diffractometer HRPD (Fischer *et al.*, 2000), installed at the Swiss Spallation Neutron Source SINQ of Paul Scherrer Institute (PSI), Switzerland. The incident neutrons of a wavelength $\lambda = 1.154$ Å were extracted from a Ge (822) monochromator with an effective intensity of 79%.

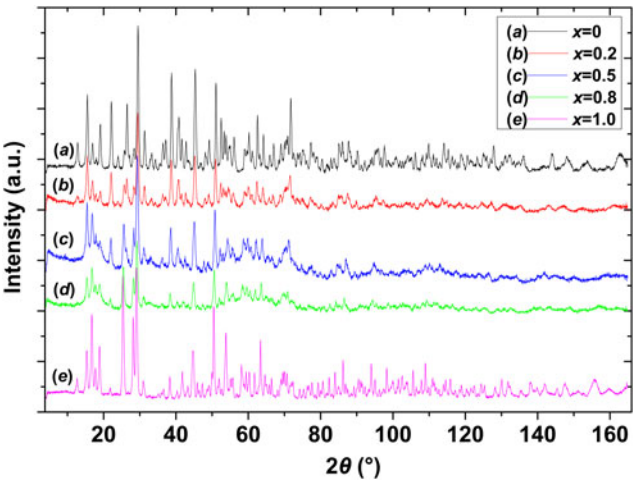

Figure 2. (Color online) NPD patterns of $LiFe_{1-x}Mn_xPO_4$ ($x = 0$, 0.2, 0.5, 0.8, and 1.0) compounds.

Data were collected over the 2θ range of 4°–165° with a step increment of 0.05°, and analyzed by the Rietveld technique (Rietveld, 1969) via the program FullProf [suite version July-2011] (Rodríguez-Carvajal, 1993, 1997). As the mean neutron scattering length of Mn (−0.373 fm) differs greatly from that of Fe (0.945 fm), the two elements mixing will cancel each other to weaken the intensity of neutron diffraction as shown in Figure 2, we collected the $LiFe_{1-x}Mn_xPO_4$ ($x = 0.5$ and 0.8) NPD data two times under the same condition.

The refinement included the five NPD data in the 2θ range of 10°–155°. The shape of the diffraction peaks were modeled by a pseudo-Voigt function and the background level was described by a 6-Coefficients polynomial function for $LiFe_{1-x}Mn_xPO_4$ ($x = 0$, 0.2, and 1.0) compounds. As the refinement of the $LiFe_{1-x}Mn_xPO_4$ ($x = 0.5$ and 0.8) data was not able to reach a convergent result with the same background level, we selected about 80 background points via user-selected by the program WinPLOTR to refine it subsequently, which proved to be very effective. The angles below 100° in 2θ (°) of $LiFe_{1-x}Mn_xPO_4$ ($x = 0$, 0.2, and 1.0) compounds and 80° of $LiFe_{1-x}Mn_xPO_4$ ($x = 0.5$ and 0.8) were, respectively, made for peak asymmetry corrections. The atomic positional parameters were refined for all atoms except Li. The isotropic displacement parameters were refined for all atoms, and finally, the occupancy parameters were refined for Li and Fe/Mn, respectively.

In order to test the possibility a mixture of site occupation of Li/Fe atoms proposed by $LiFePO_4$ NPD refined results, an XRD pattern of $LiFePO_4$ was collected on a Rint-2400 diffractometer (Rigaku Corporation) with Cu$K\alpha$ radiation. The diffraction intensity was measured from 10 to 86° using a step interval of 0.02°.

In the XRD data refinement, we first deal with the scale factor, the diffractometer zero point, the background function, and the unit-cell parameters, and then with the profile function, the atomic coordinates, and the isotropic displacement parameters, and finally, with the Li and Fe/Mn atomic occupancies deviated from nominal chemical stoichiometry. There are no excluded regions in the XRD data refinement and the limit angle for asymmetry correction is 38° for the XRD and 73° for the NPD in the Table I refinement process. The results are listed in Table I.

III. RESULTS AND DISCUSSION

Our previous investigation suggested that the kinetic property of the Mn^{2+}/Mn^{3+} redox couple is improved with forming a solid solution and a mesoporous structure and that the reversible capacity and rate performance decrease with the increase of Mn content (Zhang *et al.*, 2010, 2011).

$LiFePO_4$ NPD data were used to solve the structure by the program FOX (Favre-Nicolin and Černý, 2002) initially. *Ab initio* crystal structure solution via the program FOX indicates demonstrably that the space group of $LiFePO_4$ is *Pnma*. Thus, the olive structure of $LiFePO_4$ from Inorganic Crystal Structure Database (ICSD) was employed as the initial structure model in the following Rietveld refinement, with Li^{1+} on the 4a site and Fe^{2+} on the 4c site.

We focused on the occupancy of Li and Fe sites in $LiFePO_4$, respectively, to test the conclusion of the mixed Li/Fe occupation in a small amount in previous works (Chung *et al.*, 2008, 2012; Gardiner and Islam, 2010; Hoang and Johannes, 2011). First, all the occupancies were

https://doi.org/10.1017/S0885715614000116 Published online by Cambridge University Press

TABLE I. The occupancy results obtained from the Rietveld refinement of the $LiFePO_4$ sample.

	Occ. Li^+/Fe^{2+}	Occ. Fe^{2+}/Li^+	R_{wp} (%)	R_{exp} (%)	χ^2	R_B (%)
NPD	1.000(0)/–	1.000(0)/–	8.65	6.73	1.65	2.66
	0.85(1)/–	*0.982(4)*/–	8.54	6.74	1.61	2.66
	0.980(2)/*0.020(2)*	*0.980(2)*/*0.020(2)*	8.55	6.74	1.61	2.63
XRD	1.000(0)/–	1.000(0)/–	8.63	5.94	2.11	2.18
	1.19(3)/–	*0.976(2)*/–	8.50	5.95	2.04	2.04
	0.980(2)/*0.020(2)*	*0.980(2)*/*0.020(2)*	8.51	5.95	2.05	2.05
NPD&XRD	1.000(0)/–	1.000(0)/–	9.01/9.24	6.64/5.96	1.84/2.41	2.85/2.624
	1.07(1)/–	*0.976(2)*/–	9.12/8.93	6.67/5.95	1.87/2.25	2.93/2.30
	0.984(2)/*0.016(2)*	*0.984(2)*/*0.016(2)*	8.93/8.95	6.69/5.96	1.78/2.26	2.81/2.39

Refined parameters are in italics.

fixed to 100%, perfect chemical ordering, and the agreement between the computed and observed patterns is already good with $R_B = 2.66\%$ and $R_{wp} = 8.65\%$ ($\chi^2 = 1.65$). Then, we released to refine all the occupancies of Li and Fe sites, and found that the Li (4a) and Fe (4c) occupancy became less than full occupation, and the *R*-factors improved quite slightly to $R_B = 2.66\%$ and $R_{wp} = 8.54\%$ ($\chi^2 = 1.61$). Finally, we refined the mixture rate of Li/Fe atoms with a constraint of full occupancy in total, and the *R*-factors scarcely changed to $R_B = 2.63\%$ and $R_{wp} = 8.55\%$ ($\chi^2 = 1.61$). If the mixture of Li/Fe is true, it can be speculated that the similar result should be concluded from XRD since the X-ray atomic form factors are significantly distinguished between Li and Fe. We used the XRD data calculate as the same strategy for above. We also mixed X-rays and neutrons data for a combined refinement. The results are provided in Table I. The mean neutron-scattering length of Li (−0.190 fm) differs greatly from that of Fe (0.945 fm), so that some Fe^{2+} distributed over Li^{1+} sites will reduce the average neutron-scattering length in the Li^{1+} sites, which will decrease the result of Li^{1+} occupancy. On the contrary, the X-ray atomic form factors increase with the addition of atomic number, so that some Fe^{2+} distributed over Li^{1+} sites will increase the average atomic form factor value of XRD, which will raise the Li^{1+} occupancy and will make the occupancy value larger than 1.0 as in Table I. It seems to imply that about 2% mixed Li/Fe occupation (antisite defects) occurs, whereas the statistical *R*-factors just have a tiny improvement. The antisite defects could decrease the ionic conductivity of the cathode material and increase the polarization, because Li^{1+} ion diffusion occurs preferentially via one-dimensional channels oriented along the [010] direction (*b*-axis) (Morgan *et al.*, 2004; Islam *et al.*, 2005; Nishimura *et al.*, 2008); these antisite defects would add additional electrostatic repulsion and impede the diffusion easily. Chung *et al.* (2008, 2012) have directly demonstrated the disordered occupations by Fe atoms on Li sites in $LiFePO_4$ with high-angle annular dark-field scanning transmission electron microscopy (HAADF-STEM). An intrinsic defect type with the lowest energy is the cation antisite defect, in which Li and Fe/Mn ions exchange positions (Gardiner and Islam, 2010). The antisite exchange defects have been demonstrated theoretically for $LiMnPO_4$ and $LiFePO_4$ by M. Saiful Islam and Michelle Johannes *et al.* (Gardiner and Islam, 2010; Hoang and Johannes, 2011), respectively. The observed and calculated NPD and XRD patterns of $LiFePO_4$ are shown in Figure 3, from which it can be found that the profile calculated is statistically in agreement with the observed data.

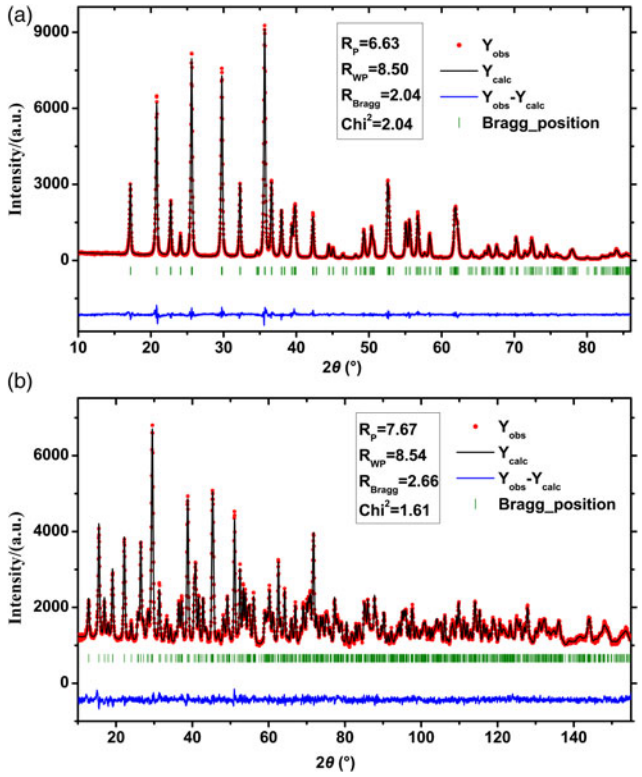

Figure 3. (Color online) Rietveld refinement on the XRD pattern (a) and NPD pattern (b) of the $LiFePO_4$ sample at room temperature. Observed intensity Y_{obs} and calculated intensity Y_{calc} are represented by red dot signs and the black solid line. The green bar represents the Bragg peaks position and the blue curve at the bottom represents the residual difference $Y_{obs} - Y_{calc}$.

It was reasonably assumed that the Mn^{2+} replacement takes place at the Fe-sites (Yao *et al.*, 2006; Molenda *et al.*, 2007; Hong *et al.*, 2011) in Rietveld refinement of $LiFe_{1-x}Mn_xPO_4$ ($x = 0$, 0.2, 0.5, 0.8, and 1.0) compounds. Table II gives the structural parameters obtained from the Rietveld refinement of the structures; some structural data obtained from the Rietveld refinement are also provided in Table III. No impurity phase was identified, and the crystal structure was successfully refined with the space group *Pnma*. The cell parameters *a*, *b*, and *c* increase linearly as the Mn content increases, inducing a linear increase in the unit-cell volume (Table III, Figure 4). This is supported by the XRD results of Padhi *et al.* (1997a). This result is reasonable since the Mn^{2+} ($r = 0.80$ Å) has a larger radius than that of the Fe^{2+} ($r = 0.74$ Å).

The selected interatomic distances and angles for all $LiFe_{1-x}Mn_xPO_4$ compounds are, respectively, described in Table III. The interatomic distances (in Å) of Li–O(2) and

https://doi.org/10.1017/S0885715614000116 Published online by Cambridge University Press

TABLE II. Structural parameters refined using the NPD data for the $LiFe_{1-x}Mn_xPO_4$ ($x = 0$, 0.2, 0.5, 0.8, and 1.0) compounds.

Atom	Site	x	y	z	B_{iso} (Å^2)	Occ
Li	4a	0	0	0	1.0(1)	0.86(2)
		0	0	0	1.4(2)	1.00(2)
		0	0	0	2.6(6)	0.96(5)
		0	0	0	2.7(6)	0.97(6)
		0	0	0	1.4(2)	0.98(1)
Fe/Mn	4c	0.28 204(9)	0.25	0.9756(3)	0.68(3)	0.982(4)/0.0
		0.2814(3)	0.25	0.9771(6)	0.53(6)	0.780(4)/0.220(4)
		0.2827(6)	0.25	0.971(2)	1.0(2)	0.528(4)/0.472(4)
		0.275(3)	0.25	0.994(8)	0.4(6)	0.228(6)/0.772(6)
		0.2816(2)	0.25	0.9726(5)	0.51(4)	0.0/0.94(1)
P	4c	0.0952(1)	0.25	0.4187(4)	0.72(2)	1.0
		0.0967(4)	0.25	0.4155(7)	0.44(4)	1.0
		0.0942(5)	0.25	0.413(2)	1.3(1)	1.0
		0.0917(7)	0.25	0.410(2)	0.8(1)	1.0
		0.0923(2)	0.25	0.4083(3)	0.59(2)	1.0
O1	4c	0.0972(2)	0.25	0.7424(4)	0.90(2)	1.0
		0.0968(4)	0.25	0.7411(7)	0.83(6)	1.0
		0.0962(6)	0.25	0.737(2)	1.5(2)	1.0
		0.0970(7)	0.25	0.733 (1)	1.2(1)	1.0
		0.0964(1)	0.25	0.7287(4)	0.87(2)	1.0
O2	4c	0.4575(1)	0.25	0.2056(4)	0.89(2)	1.0
		0.4586(2)	0.25	0.2088(8)	0.82(6)	1.0
		0.4560(5)	0.25	0.205(2)	1.2(1)	1.0
		0.4551(5)	0.25	0.211(1)	1.2(1)	1.0
		0.4551(2)	0.25	0.2110(5)	0.83(3)	1.0
O3	8d	0.1658(2)	0.0463(3)	0.2841(2)	0.94(2)	1.0
		0.1642(3)	0.0476(4)	0.2834(5)	0.66(4)	1.0
		0.1643(4)	0.0478(6)	0.2787(9)	1.4(1)	1.0
		0.1626(4)	0.0478(6)	0.2795(9)	1.1(1)	1.0
		0.1614(1)	0.0488(1)	0.2765(2)	0.86(3)	1.0

For each atom the rows are, in order (from the top): $x = 0$; $x = 0.2$; $x = 0.5$; $x = 0.8$; and $x = 1.0$, respectively.

TABLE III. Structural data of $LiFe_{1-x}Mn_xPO_4$ ($x = 0$, 0.2, 0.5, 0.8, and 1.0) compounds from the Rietveld analysis.

	$x = 0$	$x = 0.2$	$x = 0.5$	$x = 0.8$	$x = 1$
Lattice parameters					
a (Å)	10.3210(3)	10.3429(9)	10.380(2)	10.4200(9)	10.4504(2)
b (Å)	6.0035(1)	6.0224(5)	6.0492(5)	6.0800(5)	6.1051(1)
c (Å)	4.6920(1)	4.7043(4)	4.7201(4)	4.7342(4)	4.7461(1)
V (Å^3)	290.73(2)	293.02(4)	296.38(5)	299.93(4)	302.81(2)
Reliability factors					
R_{wp} (%)	8.60	12.2	11.8	16.2	10.1
χ^2	1.60	1.47	0.999	1.07	1.90
R_{Bragg} (%)	2.73	5.11	1.49	2.71	4.61
Bond lengths (Å)					
Fe(Mn)–O(1)	2.200(2)	2.209(5)	2.23(1)	2.23(4)	2.255(4)
Fe(Mn)–O(2)	2.108(2)	2.132(4)	2.109(9)	2.14(4)	2.137(4)
Fe(Mn)–O(3) × 2	2.243(2)	2.243(4)	2.262(8)	2.17(3)	2.273(3)
Fe(Mn)–O(3) × 2	2.064(1)	2.088(3)	2.091(5)	2.18(2)	2.133(2)
Fe(Mn)–P	2.835(2)	2.811(5)	2.86(1)	2.74(4)	2.862(4)
P–O(1)	1.519(3)	1.532(5)	1.529(7)	1.532(8)	1.521(3)
P–O(2)	1.536(3)	1.543(5)	1.539(7)	1.534(8)	1.541(3)
P–O(3) × 2	1.557(1)	1.536(3)	1.557(5)	1.561(5)	1.557(2)
P–Li × 2	2.662(2)	2.662(3)	2.653(4)	2.643(4)	2.648(2)
Li–O(1) × 2	2.172(1)	2.180(3)	2.198(4)	2.220(5)	2.237(2)
Li–O(2) × 2	2.086(1)	2.080(3)	2.107(4)	2.098(5)	2.105(1)
Li–O(3) × 2	2.187(2)	2.178(3)	2.172(4)	2.169(4)	2.158(1)
Bond angles (°)					
O(2)–Fe(Mn)–O(3)	89.9(1)	89.5(2)	90.1(4)	88(2)	89.7(2)
O(3)–Fe(Mn)–O(3)	119.0(1)	118.3(3)	119.0(3)	112.7(8)	117.6(1)
O(1)–P–O(2)	113.1(2)	112.3(4)	111.9(6)	114.0(7)	113.2(2)
O(2)–P–O(3)	106.2(2)	105.5(3)	106.8(5)	107.0(5)	106.5(1)
O(3)–P–O(3)	103.5(1)	105.0(3)	103.5(4)	103.9(4)	104.2(1)

https://doi.org/10.1017/S0885715614000116 Published online by Cambridge University Press

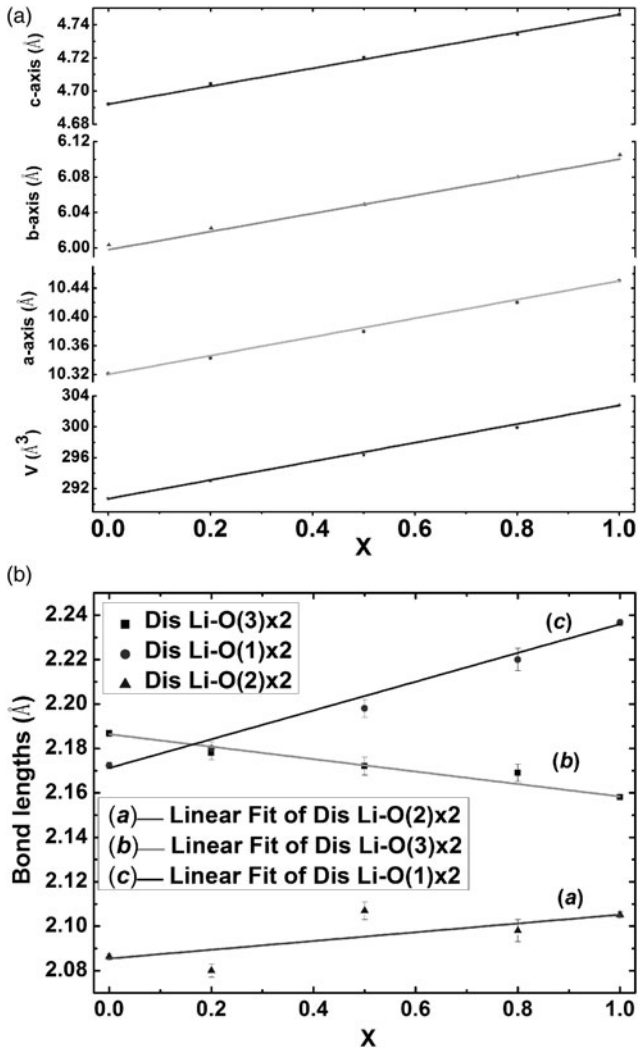

Figure 4. Structural data of $LiFe_{1-x}Mn_xPO_4$ ($x = 0$, 0.2, 0.5, 0.8, and 1.0) compounds. The lattice parameters of olivine phase for $LiFe_{1-x}Mn_xPO_4$ ($x = 0$, 0.2, 0.5, 0.8, and 1.0) compounds increase linearly as a function of Mn content (x) (a) and the interatomic distances (in Å) of Li–O(2) and Li–O(1) increase, while the interatomic distances (in Å) of Li–O(3) decrease on the addition of Mn (b).

Li–O(1) increase while the interatomic distances (in Å) of Li–O(3) decrease on the addition of Mn (Figure 4), respectively, which partially explains a higher potential plateau of ~4.1 eV in $LiMnPO_4$ than ~3.5 eV in $LiFePO_4$. An XRD study of $LiFe_{1-x}Mn_xPO_4$ interatomic distance was not able to demonstrate a linear relationship described by Yao *et al.* (2006), because the X-ray is scattered by the extranuclear electron density, but the neutrons are by the nuclei. The Li^{1+} ion diffusion occurs preferentially via one-dimensional channels oriented along the [010] direction (b-axis) (Morgan *et al.*, 2004; Islam *et al.*, 2005; Nishimura *et al.*, 2008); so the interatomic distances (in Å) of Li–O(3) decrease while the cell parameters increase, which will make the Li^{1+} ion diffusion become difficult. As a result, $LiMnPO_4$ has a higher potential plateau than $LiFePO_4$, consistent with our previous investigated electrochemical behaviors (Zhang *et al.*, 2010, 2011).

IV. SUMMARY

Five different phase-pure compositions of $LiFe_{1-x}Mn_xPO_4$ ($x = 0$, 0.2, 0.5, 0.8, and 1.0) have been synthesized and studied by NPD. Rietveld refinements (FullProf program suite version July-2011) for the NPD and XRD profiles measured for $LiFePO_4$, respectively, show that about 2% Fe^{2+} may distribute over Li^{1+} sites, which could decrease the ionic conductivity of the cathode material and increase the polarization. The a, b, and c cell parameters increase linearly, and the interatomic distances (in Å) of Li–O(2) and Li–O(1) increase, while the interatomic distances (in Å) of Li–O(3) decrease with the addition of Mn, respectively. The interatomic distances (in Å) of Li–O(3) decrease will also make the Li^{1+} ion diffusion more difficult.

ACKNOWLEDGEMENTS

The authors are indebted to Dr. D. Sheptyakov of SINQ/PSI, Switzerland, for his help in neutron diffraction experiment. Financial support from "973" project (Grant No. 2010CB833102) is acknowledged. This work was also supported by the National Natural Science Foundation of China (NSFC) Grant No. 11174334 and CAS innovation project (Grant No. KJCX2-YW-W26).

SUPPLEMENTARY DATA

CIF files pertaining to the compounds described have been deposited with ICDD®. For information please contact info@icdd.com.

Amine, K., Yasuda, H., and Yamachi, M. (**2000**). "Olivine $LiCoPO_4$ as 4.8 V electrode material for lithium batteries," Electrochem. Solid-State Lett. **3**(4), 178–179.

Armand, M. and Tarascon, J.-M. (**2008**). "Building better batteries," Nature **451**, 652–657.

Chung, S. Y., Blocking, J. T., and Chiang, Y. M. (**2002**). "Electronically conductive phosphor-olivines as lithium storage electrodes," Nature Mater. **1**, 123–128.

Chung, S. Y., Choi, S. Y., Yamamoto, T., and Ikuhara, Y. (**2008**). "Atomic-scale visualization of antisite defects in $LiFePO_4$," Phys. Rev. Lett. **100**, 125502-1–125502-4.

Chung, S. Y., Choi, S. Y., Lee, S., and Ikuhara, Y. (**2012**). "Distinct configurations of antisite defects in ordered metal phosphates: comparison between LiMnPO4 and $LiFePO_4$," Phys. Rev. Lett. **108**, 195501-1–195501-5.

Dominko, R., Gaberscček, M., Drofenik, J., Bele, M., and Pejovnik, S. (**2001**). "A novel coating technology for preparation of cathodes in Li-Ion batteries," Electrochem. Solid-State Lett. **4**(11), A187–A190.

Favre-Nicolin, V. and Černý, R. (**2002**). "FOX, 'free objects for crystallography': a modular approach to *ab initio* structure determination from powder diffraction," J. Appl. Crystallogr. **35**, 734–743.

Fischer, P., Frey, G., Koch, M., Könnecke, M., Pomjakushin, V., Schefer, J., Thut, R., Schlumpf, N., Bürge, R., Greuter, U., Bondt, S., and Berruyer, E. (**2000**). "High-resolution powder diffractometer HRPT for thermal neutrons at SINQ," Physica B **276–278**, 146–147.

Gardiner, G. R. and Islam, M. S. (**2010**). "Anti-site defects and ion migration in the $LiFe_{0.5}Mn_{0.5}PO_4$ mixed-metal cathode material," Chem. Mater. **22**, 1242–1248.

Hoang, K. and Johannes, M. (**2011**). "Tailoring native defects in $LiFePO_4$: insights from first-principles calculations," Chem. Mater. **23**, 3003–3013.

Hong, J., Wang, F., Wang, X. L., and Graetz, J. (**2011**). "$LiFe_xMn_{1-x}PO_4$: a cathode for lithium-ion batteries," J. Power Sources **196**, 3659–3663.

Huang, H., Yin, S. C., and Nazar, L. F. (**2001**). "Approaching theoretical capacity of $LiFePO_4$ at room temperature at high rates," Electrochem. Solid-State Lett. **4**, A170–A172.

Islam, M., Driscoll, D., Fisher, C., and Slater, P. (**2005**). "Atomic-scale investigation of defects, dopants, and lithium transport in the $LiFePO_4$ olivine-type battery material," Chem. Mater. **17**, 5085–5092.

Li, G. H., Azuma, H., and Tohda, M. (**2002**). "$LiMnPO_4$ as the cathode for lithium batteries," Electrochem. Solid-State Lett. **5**(6), A135–A137.

https://doi.org/10.1017/S0885715614000116 Published online by Cambridge University Press

Li, H., Wang, Z. X., Chen, L. Q., and Huang, X. J. (**2009**). "Research on advanced materials for Li-ion batteries," Adv. Mater. **21**, 4593–4607.

Molenda, J., Ojczyk, W., and Marzec, J. (**2007**). "Electrical conductivity and reaction with lithium of $LiFe_{1-y}Mn_yPO_4$ olivine-type cathode materials," J. Power Sources **174**, 689–694.

Morgan, D., Van der Ven, A., and Ceder, G. (**2004**). "Li conductivity in Li_xMPO_4 (M = Fe, Mn, Co, Ni) olivine materials," Electrochem. Solid-State Lett. **7**(2), A30–A32.

Nishimura, S., Kobayama, G., Ohoyama, K., Kanno, R., Yashima, M., and Yamada, A. (**2008**). "Experimental visualization of lithium diffusion in Li_xFePO_4," Nature Mater. **7**, 707.

Padhi, A. K., Nanjundaswamy, K. S., and Goodenough, J. B. (**1997a**). "Phospho-olivines as positive-electrode materials for rechargeable lithium batteries," J. Electrochem. Soc. **144**, 1188–1194.

Padhi, A. K., Nanjundaswamy, K. S., Masquelier, C., Okada, S., and Goodenough, J. B. (**1997b**). "Effect of structure on the Fe^{3+}/Fe^{2+} redox couple in iron phosphates," J. Electrochem. Soc. **144**, 1609–1613.

Rietveld, H. M. (**1969**). "A profile refinement method for nuclear and magnetic structures," J. Appl. Crystallogr. **2**, 65–71.

Rodríguez-Carvajal, J. (**1993**). "Recent advances in magnetic structure determination by neutron powder diffraction," Physica B **192**, 55–69.

Rodríguez-Carvajal, J. (**1997**). *Fullprof, program for rietveld refinement* (Laboratories Léon Brillouin (CEA-CNRS), Saclay, France).

Streltsov, V. A., Belokoneva, E. L., Tsirelson, V. G., and Hansen, N. K. (**1993**). "Multipole analysis of the electron density in triphylite, $LiFePO_4$, using X-ray diffraction data," Acta Crystallogr. B **49**(2), 147–153.

Tarascon, J.-M. and Armand, M. (**2001**). "Issues and challenges facing rechargeable lithium batteries," Nature **414**, 35–367.

Wang, D. Y., Li, H., Shi, S. Q., Huang, X. J., and Chen, L. Q. (**2005**). "Improving the rate performance of $LiFePO_4$ by Fe-site doping," Electrochem. Acta **50**, 2955–2958.

Wolfenstine, J. and Allen, J. (**2005**). "Ni^{3+}/Ni^{2+} redox potential in $LiNiPO_4$," J. Power Sources **142**, 389–390.

Yamada, A., Chung, S., and Hinokuma, K. (**2001**). "Optimized $LiFePO_4$ for lithium battery cathodes," J. Electrochem. Soc. **148**, A224–A229.

Yao, J., Bewlay, S., Konstantionv, K., Drozd, V. A., Liu, R. S., Wang, X. L., Liu, H. K., and Wang, G. X. (**2006**). "Characterisation of olivine-type $LiMn_xFe_{1-x}PO_4$ cathode materials," J. Alloys Compd **425**, 362–366.

Zhang, B., Wang, X. J., Liu, Z. J., and Huang, X. J. (**2010**). "Enhanced electrochemical performances of carbon coated mesoporous $LiFe_{0.2}Mn_{0.8}PO_4$," J. Electrochem. Soc. **157**, A285–A288.

Zhang, B., Wang, X. J., Liu, Z. J., and Huang, X. J. (**2011**). "Electrochemical performances of $LiFe_{1-x}Mn_xPO_4$ with high Mn content," J. Power Sources **196**, 6992–6996.

Zhou, F., Cococcioni, M., Kang, K., and Ceder, G. (**2004**). "The Li intercalation potential of $LiMPO_4$ and $LiMSiO_4$ olivines with M = Fe, Mn, Co, Ni," Electrochem. Commun. **6**, 1144–1148.